Trajectory-tracking control of a planar parallel robot using generalized predictive control with constraints

Trajectory-tracking control of a planar parallel robot using generalized predictive control with constraints

M Rodelo[1], J L Villa[2], and E Yime[3]

[1] Universidad Simón Bolívar, Barranquilla, Colombia
[2] Universidad Tecnológica de Bolívar, Cartagena de Indias, Colombia
[3] Universidad del Atlántico, Barranquilla, Colombia

E-mail: mrodelo4@unisimonbolivar.edu.co

Abstract. This paper presents the generalized predictive control with constraints, implemented to a planar parallel robot in order to calculate and track the desired trajectory of the end-effector of this robot. The manipulator is driven by three brushless direct current motors, and each one has an encoder to measure the velocity and rotation angles of the motors. Three constraints were considered to interact with the control law: control signal, terminal response and the over impulse constraints. The performance of the control law is evaluated in the simulation environment using Matlab/Simulink with the physic model developed through simscape multibody. The angular position and velocity errors for each of the three motors were calculated. Likewise, the output torques for each one were estimated. The results proved that the control law proposed with the constraints imposed for each motors has a good efficiency with a stable response time of the robot in performing the trajectory tracking, contributing to the scientific community a strategy of predictive optimization of control actions with multiple constraints applied on parallel robots.

1. Introduction

Parallel robots have been a trend in the development of theoretical research and industrial applications as a result of their advantages over serial manipulator architectures [1]. Compared to conventional serial manipulators, parallel robots have some advantages, such as high structural stiffness, lightness, high load capacity, good dynamic properties and precise motion control [2].

A literature review show a large number of papers dedicated to the study of the control of parallel robot, as: Glazunov *et al.*, used a spherical mechanism of parallel structure containing three kinematic chains and performing spherical motions, where the velocity analysis was necessary to control the robot and its dynamic analysis, with successfully results [3]. Liang *et al.*, developed a research on the intelligent recognition system using a parallel robot (Gough-Stewart) and sliding mode controller for the control of this robot. The results prove the validity of the dynamic model and the stability of control system [4, 5]. khalapyan *et al.*, developed a model of planar 3-RPR mechanism with an electric drive based on a direct current (DC) motor. The results it allowed to determine the necessary distance of the trajectory of the parallel structure of the robot from the theoretical limits of its workspace [6].

In this paper, the generalized predictive control strategy with constraints is implemented to the planar 3-RRR parallel robot with three degrees of freedom, for tracking a classical circular trajectory. This paper is organized as follows, section 2, show a brief description of Brushless

DC motor modelling. Section 3 provides the generalized predictive control with constraints; the results are presented in section 4. The section 5 summarizes the significant conclusions and research future.

2. Brushless direct current motor modeling

A Brushless direct current (BLDC) motor is a class of electrical machines that converts direct current electrical power into mechanical power. For the purpose of the controller design, it is necessary to know the mathematical model of the BLDC motors [7]. Figure 1, illustrates the electrical equivalent scheme of BLDC motor. From the analysis of Figure 1, the electrical and mechanical performance of the BLDC motor are determined by equations Equation (1) and Equation (2) respectively.

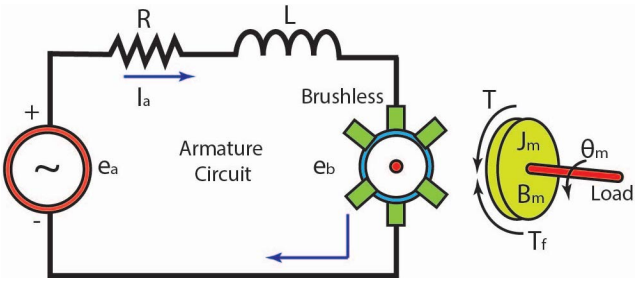

Figure 1. Electrical equivalent of BLDC motor.

$$e_a(t) = R_a I_a(t) + L\frac{dI_a(t)}{dt} + e_b(t), \tag{1}$$

$$T(t) = J_m\frac{d\omega_m(t)}{dt} + B_m\ \omega_m(t). \tag{2}$$

The generalized transfer function with load and gearbox is given by Equation (3), and is represented with the block diagram illustrated in Figure 2. Where the signals that interact in the motor are shown. From the input voltage to the output torque on the shaft, essential for control loop development.

$$\frac{\Theta_{L(s)}}{E_{a(s)}} = \frac{K_T[N_1/N_2]}{LJ_mS^3 + (RJ_m + B_mL)S^2 + (K_TK_E + RB_m)S}. \tag{3}$$

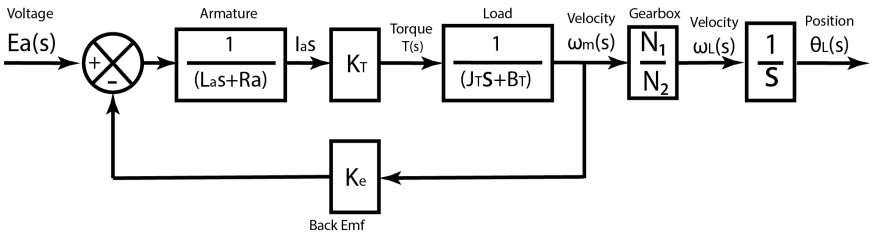

Figure 2. Block diagram of BLDC Motor.

3. Generalized predictive control

Based on [8], the fundamental idea of the generalized predictive control (GPC) is determine a sequence of future control actions in order to minimizes a multi-stage cost function defined over a prediction horizon [9]. The index to be minimized is a quadratic function that measures on distance between the predicted output of the system and a reference path to prediction horizon, considering the control effort required to obtain that output [10].

3.1. Generalized predictive control formulation

For the GPC modelling, a structure of a controller auto-regressive integrated moving-average (CARIMA) model is used [11], which is given by a transfer function along with an additional term that represents a disturbance. Consider an single-input, single-output (SISO) discrete-time system, as follow in Equation (4).

$$A(z^{-1})y(t) = B(z^{-1})z^{-d}u(t-1) + C(z^{-1})\frac{e(t)}{\triangle}, \tag{4}$$

where, $\triangle = 1 - z^{-1}$ A, B and C are the following polynomials on the reverse displacement operator z^{-1}, and d is the dead time of the system, as show in Equation (5).

$$\begin{array}{l} A(z^{-1}) = 1 + a_1 z^{-1} + a_2 z^{-2} + ... + a_{na} z^{-na}, \\ B(z^{-1}) = b_0 + b_1 z^{-1} + b_2 z^{-2} + ... + b_{nb} z^{-nb}, \\ C(z^{-1}) = c_0 + b_1 z^{-1} + c_2 z^{-2} + ... + c_{nc} z^{-nc}. \end{array} \tag{5}$$

3.2. Cost function and optimal prediction

In accordance to GPC algorithm, the control sequence that minimizes the multistage cost function [12], is solved as shown in Equation (6).

$$J = \sum_{j=N_1}^{N_2} \delta(j)[\hat{y}(t+j|t) - w(t+j)]^2 + \sum_{j=1}^{N_u} \lambda(j)[\triangle u(t+j-1)]^2. \tag{6}$$

The objective is to calculate the future $u(t)$, $u(t+1)$,...control sequence so that the future output of process $y(t+j)$ remains close to $w(t+j)$. This is achieved by minimizing J; to compute the predicted output, consider the following Diophantine function [13], as show in Equation (7).

$$1 = E_j(z^{-1})\tilde{A} + z^{-j}F_j(z-1), \tag{7}$$

where, $\tilde{A} + z^{-1} = \triangle A z^{-1}$; the polynomials E_j and F_j can be obtained by dividing 1 between $\tilde{A}(z^{-1})$ and the result can be factored as z^{-j}. Therefore, the division quotient is then the polynomial $E_j(z^{-1})$. As the degree of polynomial $E_j(z^{-1})$ is equal to $j-1$, the terms of noise are found in the future. Thus, the best prediction of $y(t+j)$ will be Equation (8).

$$\hat{y}(t+j|t) = G_j(z^{-1})\triangle u(t+j-d-1) + F_j(z^{-1})y(t), \tag{8}$$

where, $G_j(z^{-1}) = E_j(z^{-1})\ B(z^{-1})$; therefore, the optimal set of predictions j is given by Equation (9).

$$\begin{array}{c} \hat{y}(t+d+1|t) = G_{d+1}\triangle u(t) + F_d + 1y(t), \\ \hat{y}(t+d+2|t) = G_{d+2}\triangle u(t+1) + F_d + 2y(t), \\ \vdots \\ \hat{y}(t+d+N|t) = G_{d+N}\triangle u(t+N) + F_d + Ny(t). \end{array} \tag{9}$$

Equation (9) can be written in matrix form, as note in Equation (10).

$$y = Gu + F(z^{-1})y(t) + G'(z^{-1})\triangle u(t-1), \tag{10}$$

where, each term in Equation (10) is a matrix that defines the output or prediction, y, future controls, U, past controls, F, and disturbances, G, as shown in Equation (11).

$$y = \begin{bmatrix} \hat{y}(t+d+1|t) \\ \hat{y}(t+d+2|t) \\ \vdots \\ \hat{y}(t+d+N|t) \end{bmatrix}, \; U = \begin{bmatrix} \triangle u(t) \\ \triangle u(t+1) \\ \vdots \\ \triangle u(t+N-1) \end{bmatrix}, \; G = \begin{bmatrix} g_0 & 0 & \dots & 0 \\ g_1 & 0 & \dots & 0 \\ \vdots & \vdots & \ddots & \vdots \\ g_{N-1} & g_{N-2} & \cdots & g_0 \end{bmatrix},$$

$$F(z^{-1}) = \begin{bmatrix} F_{d+1}(z^{-1}) \\ F_{d+2}(z^{-1}) \\ \vdots \\ F_{d+N}(z^{-1}) \end{bmatrix}, \; G'(z^{-1}) = \begin{bmatrix} z(G_{d+1}(z^{-1}) - g_0) \\ z^2(G_{d+2}(z^{-1}) - g_0 - g_1 z^{-1}) \\ \vdots \\ z^N(G_{d+N}(z^{-1}) - g_0 - g_1 z^{-1} - \\ \cdots - g_{N-1} z^{-(N-1)}) \end{bmatrix}. \tag{11}$$

3.3. Constraints

In this research it is considered that in every process there are operating limits for safety, environment and equipment used, such as motors, sensors, response speed, etc [14]. The three constraints considered in this research are:

3.3.1. Control signal constraint. The first constraint concerns the controller and its limitations applied on tracking-trajectory of the end-effector; therefore, the constraint is given by Equation(12).

$$u_{min} \leq u(k) \leq u_{max}, \quad \forall k \in [0, N_{u-1}]. \tag{12}$$

3.3.2. Terminal constraint. Second, a terminal constraint is evaluated at the end of the control horizon, where a specific trajectory performance of the mobile platform is present, and $y(k)$=$w(k)$. This ensures that the expected performance will track the reference or set point provided under an established control condition; thus, the system output is represented by Equation (13).

$$\begin{gathered} y = w, \\ y(k+N_2) = w(k+N_2), \\ y = G\triangle u + f. \end{gathered} \tag{13}$$

3.3.3. Over impulse constraint. Finally, in case that the two previous constraints do not consider the desired trajectory change caused by some disturbances; therefore, this restriction will only work if the path is modified by an unexpected impulse (torque), as given by Equation (14).

$$y(k) \leq w(k) \; or \; y(k) \geq w(k), \; \forall k \in [N_1 N_2]. \tag{14}$$

If the reference is positive, the variable must always be smaller than the reference; if the reference is negative, the variable will be greater than the reference; so the constraint will always depend on the direction of the reference; therefore the constraint is denoted by Equation (15).

$$\begin{bmatrix} G \\ \dots \\ -G \end{bmatrix} \triangle u \leq \begin{bmatrix} 1w(k-f) \\ \dots \\ -1w(k+f) \end{bmatrix}. \tag{15}$$

3.4. Control law

The control law or cost function can be written as shown in the Equation (16).

$$J = (Gu + f - W)^T (Gu + f - W) + \lambda u^T u. \tag{16}$$

By rearranging the terms of Equation (16) and removing the terms that do not depend on u, Equation (17) was obtained, as follow.

$$J = u^T \{G^T \delta G + \lambda\} u + 2(f - w)^T \delta G u, \tag{17}$$

where, $H = G^T \delta G + \lambda$, represents the Hessian matrix and $C = G^T \delta (f - w)$, denotes the gradient C. For this research the problem of optimization with a quadratic objective and linear inequalities (constraints) has been defined as a quadratic problem, as denoted in Equation (18).

$$\min_{\triangle u(t)} J, \quad Subject\ to,\ C^u \triangle u(t) \geq C(t + \frac{1}{t}), \tag{18}$$

where C^u, combines all matrices on the left side of the inequality, and $C(t + \frac{1}{t})$ on the right side contains all error vectors of the constraint equation.

4. Results

The prototype of the planar 3-RRR parallel robot was modeled in the computer-aided design (CAD) software Solidworks (see Figure 3(a)), and built according to technical specifications, as show in Figure 3(b). The robotic system uses three Maxon Ec-i motors with a diameter of 52 mm, brushless, 180 W, with halls sensors and encoders with 1024 pulses per revolution. Each motor is coupled to a 4-30 nm Maxon gearbox in ceramic version, and is connected to an Epos 2 70/10 controller. The rotating angles of the motors are measured and are treated as feedback signals. The control is dominated by an individual controller. The difference of a command signal and a feedback encoder signal is treated as an input of a controller. The controller outputs drive the three motors.

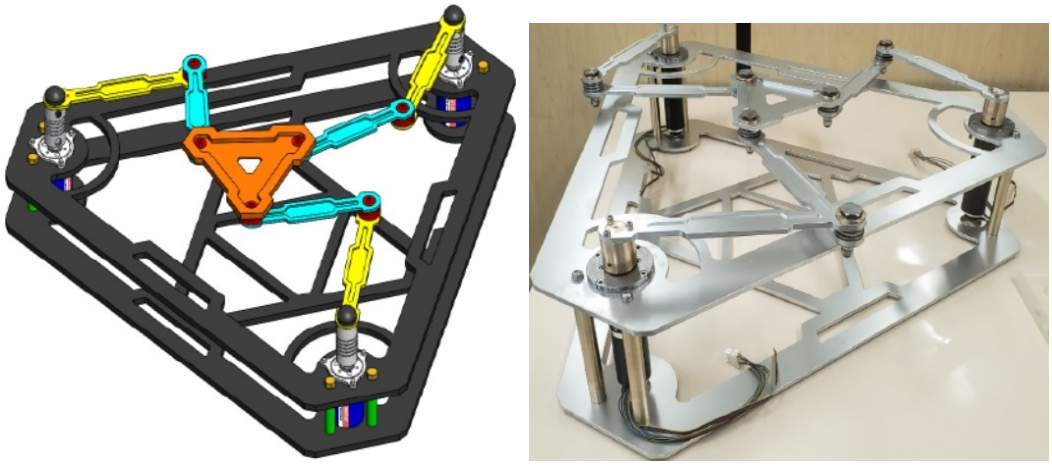

(a) (b)

Figure 3. (a) CAD modelling, and (b) prototype of a planar 3RRR parallel robot.

The validation for the kinematics, dynamics and control law were developed in MATLAB environment. Figure 4(a), shows the control scheme built in Matlab-Simulink with its correlation with the kinematics and dynamics. For dynamic model it was used the package Matlab-Simscape multibody with the purpose of setting the output torques for each motor, as observed in Figure 4(b). On the other hand, the trajectory-tracking is a classical circular motion with constant orientation in the XY plane. Likewise, in order to validate the interactions of the GPC, a simulation based on the response to the step was developed, considering the dynamic model of the BLDC motors. For this, it was necessary to solve the transfer function as shown in section 2, as denoted Equation (19). The position control of the manipulator for a circular trajectory, and the simulation results are good in agreement.

$$G_s = \frac{K_P}{S(T_pS+1)}e^{-T_ds}, \tag{19}$$

where, K_p= 2, T_p= 0.04 and T_d= 0.5; therefore, we proceed to discretized the transfer function, with a sampling period of 0.1 s and a zero order retainer, through the Matlab c2d function, as follow in Equation (20).

$$G(z^{-1}) = \frac{0.2448Z^{-1} + 0.2448Z^{-2}}{1 - 1.755Z^{-1} + Z^{-2}}. \tag{20}$$

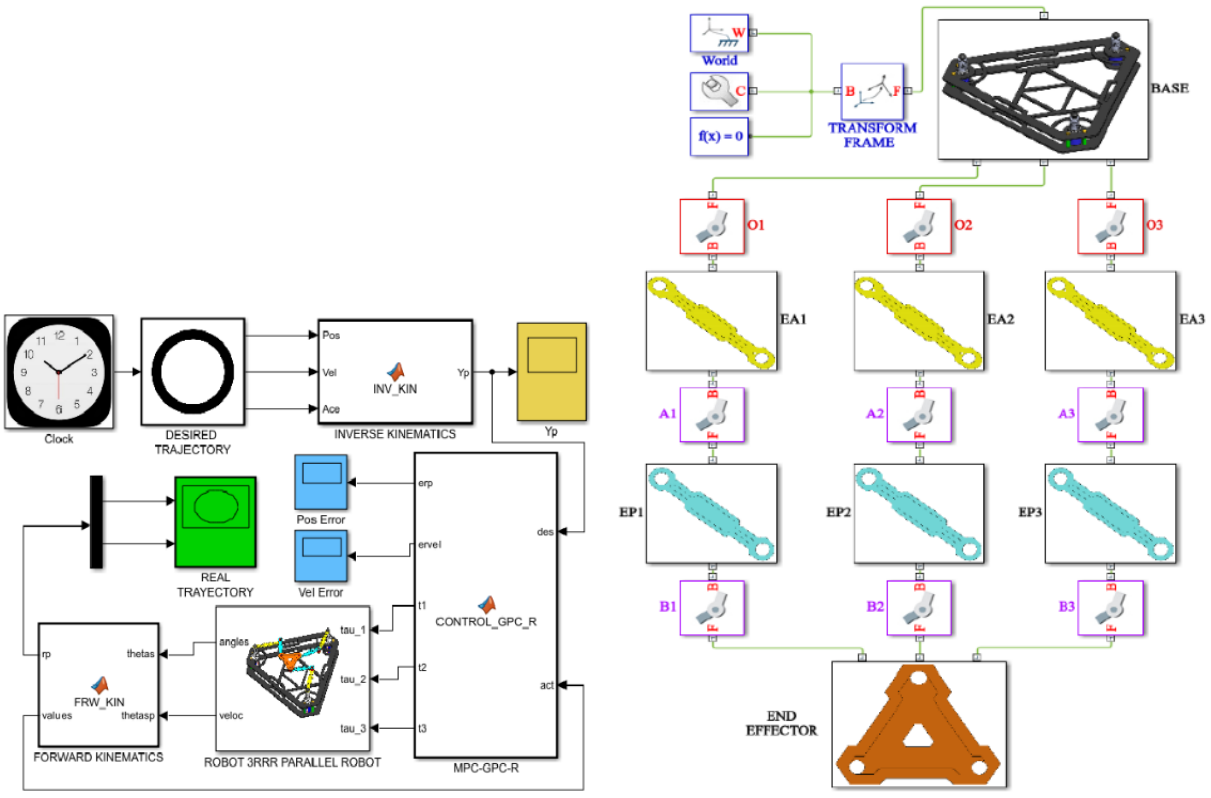

(a) (b)

Figure 4. (a) Block diagram in MATLAB/Simulink, and (b) dynamic modelling in MATLAB/Simscape multibody.

Results show that the workspace trajectories are closer to reference using GPC controller without constraints, as observed in Figure 5(a); however, GPC-R controllers improve the tracking

of the workspace trajectory in presence of disturbances, since with this controller the robot softly follows the abrupt changes in direction, because to the anticipative effect of the predictive control, as shown in Figure 5(b). Likewise, it is observed that the simulation of the BLDC motor, is subjected by increasing the control effort, the error in the system decreases and vice-versa, and the constraints imposed in the algorithm are not exceeded in any case, successfully reaching the desired reference. Finally, in order to develop the position and velocity errors of the three actuators of robot over a trajectory the root mean square error (RMSE) of the actuators [15], is considered and calculated using Equation (21). Where, $e(t)$ is the error vector of the three motors for each t instant.

$$RMSE(e) = \frac{1}{3m}\sum_{t=1}^{m}\sqrt{e(t)^T e(t)}. \tag{21}$$

The maximum tracking position and velocity error for each motors related to the set point does not exceed 0.05 rad and 0.25 rad/s, after 10 s, respectively. Furthermore, the maximum torques at three motors were -0.9 Nm, -0.5 Nm and -0.7 Nm for joints A_1, A_2 and A_3, respectively.

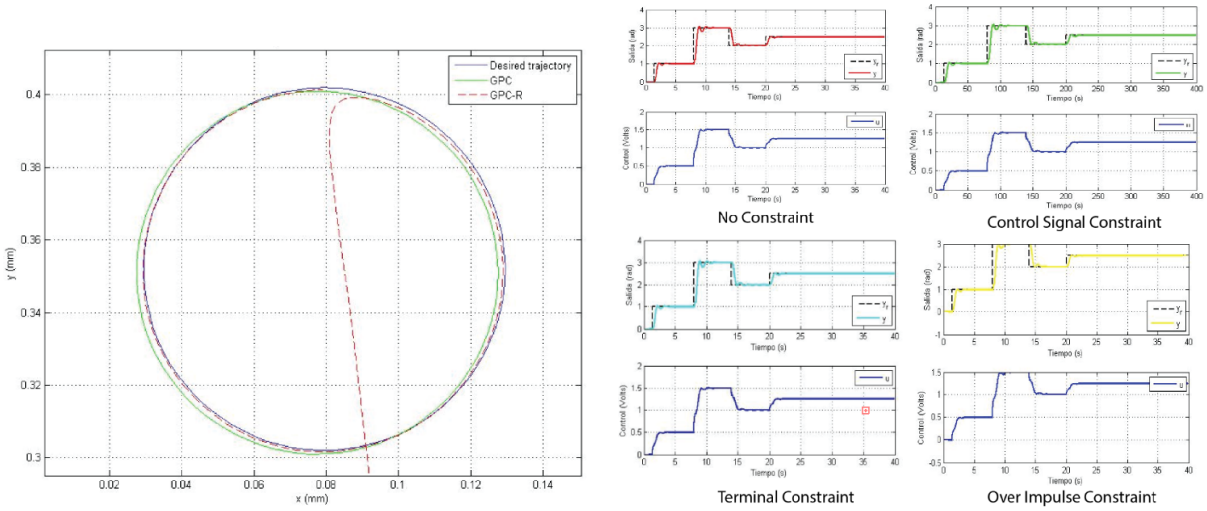

(a) (b)

Figure 5. (a) Workspace trajectories, and (b) GPC controllers under step response.

5. Conclusion

In this paper we have presented a trajectory-tracking control scheme of a 3-DOF 3-RRR planar parallel manipulator using GPC. The results show that the design can successfully perform the position control of the manipulator for a classical circular trajectory implementing a GPC controllers with three types of constraints. This type of control could be extended in applications where high precision and reliability are required, even in presence of disturbances that affect the controllability and stability, as in rehabilitation robotics where this prototype will be evaluated in future research.

References

[1] Artemov D V, Masyuk V M, Orekhov S Y, Pchelkina I V 2019 *IOP Conference Series: Materials Science and Engineering* **489** 012052:1
[2] Yime E, Roldán J, Villa J 2017 *Prospectiva* **15(2)** 85
[3] Glazunov V A, Filippov G S, Rashoyan G V, Aleshin A K, Shalyukhin K A, Skvortsov S A, Antonov A V, Terekhova A N 2019 *Journal of Physics: Conference Series* **1260** 112012:1

[4] Liang Chen L, Sun H, Jia Q, Yu T, Zhao W 2020 *Journal of Physics: Conference Series* **1550** 042040:1
[5] Chen L, Sun H, Jia Q, Zhang Y, Cao S, Zhao W, Yu T 2020 *Journal of Physics: Conference Series* **1518** 012058:1
[6] Khalapyan S Y, Rybak L A, Kuzmina V S, Kholoshevskaya L R, Ignatov A D, Popov M V 2020 *Journal of Physics: Conference Series* **1582** 012074:1
[7] Zhang D, Wang J 2019 *Journal of Physics: Conference Series* **1303** 012124:1
[8] Kiselev A, Kuznietsov A, Leidhold R 2018 Performance investigation of generalized predictive position control for a PMSM in view of reference trajectory tracking *IEEE International Conference on Industrial Technology (ICIT)* (Lyon: IEEE)
[9] Lara-Molina F A, Rosario J M, Dumur D, Wenger P 2012 Generalized predictive control of parallel robots *Robot Motion and Control 2011* vol 422, ed Kozłowski K (London: Springer)
[10] Zenan C, Wei W, Di W 2020 *Journal of Physics: Conference Series* **1486** 072003:1
[11] Xu J, Pan X, Li Y, Wang G, Martínez R 2019 *Journal of Difference Equations and Applications* **25(9-10)** 1255
[12] Zhang C, Liu B 2020 *IOP Conference Series: Materials Science and Engineering* **784** 012034:1
[13] Rahmawati R, Sugandha A, Tripena A, Prabowo A 2019 *Journal of Physics: Conference Series* **1179** 012001:1
[14] Yao X, Yang G 2015 Constrained generalized predictive control for propulsion motor of autonomous underwater vehicle *International Conference on Control, Automation and Information Sciences (ICCAIS)* (Changshu: IEEE)
[15] Hazry D, Sugisaka M 2006 Proportional control for trajectory tracking of a wheeled mobile robot *SICE-ICASE International Joint Conference* (Busan: IEEE)